Internet Appendix for

"Options on Interbank Rates and Implied Disaster Risk"

A Literature review

We provide detailed comparisons with related papers in three tables, highlighting our modeling innovations and empirical contributions. The first table juxtaposes our model and existing models of time-varying disaster risk. This comparison clearly shows how our work builds upon and differentiates itself from the existing literature. Notably, it emphasizes the reduced-form nature of our model, distinguishing it from equilibrium models. Additionally, the table shows that our parameter choices are estimated rather than calibrated. Our model also focuses on different asset classes, in contrast to prior models that are calibrated to match equity market moments.

	Model type	Parameter choices	Extracting disaster risk	Target asset classes
This paper	Reduced-form	Estimation	Yes	Interbank lending, caps, swaptions, nominal government bonds
Gabaix (2012)	Equilibrium	Calibration	No	Equity market, equity index options, nominal government/corporate bonds
Wachter (2013)	Equilibrium	Calibration	Yes	Equity market
Tsai (2015)	Equilibrium	Calibration	Yes	Equity market, nominal government bonds
Seo and Wachter (2018)	Equilibrium	Calibration	Yes	Equity market, equity index options, CDX tranches

The second table compares different ways in which time-varying disaster risk is characterized in the literature. Our relative advantage is that we can identify and extract the short-run

and long-run components of disaster risk, providing a more nuanced understanding of risk dynamics.

	How time-varying disaster risk is characterized
This paper	The short-run and long-run components of disaster risk are filtered through the unscented Kalman filter from interbank rates and options.
Berkman, Jacobsen, and Lee (2011)	A crisis severity index is constructed based on the number of international political crises.
Manela and Moreira (2017)	A disaster concern measure, called News implied volatility (NVIX), is calculated using textual analysis of newspaper articles.
Bakshi, Gao, and Xue (2023)	The disaster probability is computed from put option prices by solving a minimum discrepancy problem for the pricing kernel.

The third table compares our paper with prior studies on interest rate options. The table highlights that our model incorporates both stochastic volatility and jump components. It also juxtaposes the number of observable and unobservable state variables in each paper's main model. The empirical methodologies are also summarized in the table, in terms of the filtering method, option pricing approach, and types of interest rate options used in the analyses.

	Stochastic volatility	Jump	Number of state variables		Filtering	Option pricing	Types of interest rate options
			Observable	Unobservable			
This paper	Yes	Yes	1	4	Unscented Kalman filter	Close-form solution	ATMF swaptions and caps
Longstaff, Santa-Clara, and Schwartz (2001)	No	No	0	4	Eigenvalue calculation	Simulation-based pricing	ATMF swaptions and caps
Han (2007)	Yes	No	0	3	Matching with observed prices	Close-form solution	ATMF swaptions and caps
Trolle and Schwartz (2009)	Yes	No	0	3	Extended Kalman filter	Close-form solution	ATMF swaptions and ATM, OTM and ITM caps
Bakshi, Crosby, Gao, and Hansen (2023)	Yes	No	0	5	Unscented Kalman filter	Simulation-based pricing	Treasury options

B Unscented Kalman filter

As discussed in Section 3.2, we derive the discrete-time state equation based on the exact relation between $S_t = [\lambda_t, \xi_t, \mu_t, x_t]^\top$ and $S_{t-\Delta t} = [\lambda_{t-\Delta t}, \xi_{t-\Delta t}, \mu_{t-\Delta t}, x_{t-\Delta t}]^\top$. To do so, we first integrate both sides of the stochastic differential equations for λ_t, ξ_t, μ_t, and x_t from time $t - \Delta t$ to time t:

$$\begin{aligned}
\lambda_t &= \lambda_{t-\Delta t} + \kappa_\lambda \int_{t-\Delta t}^{t} (\xi_u - \lambda_u) du + \sigma_\lambda \int_{t-\Delta t}^{t} \sqrt{\lambda_u} dB_{\lambda,u}, \\
\xi_t &= \xi_{t-\Delta t} + \kappa_\xi \int_{t-\Delta t}^{t} (\bar{\xi} - \xi_u) du + \sigma_\xi \int_{t-\Delta t}^{t} \sqrt{\xi_u} dB_{\xi,u}, \\
\mu_t &= \mu_{t-\Delta t} + \kappa_\mu \int_{t-\Delta t}^{t} (\bar{\mu} - x_u) du + \sigma_\mu \int_{t-\Delta t}^{t} dB_{\mu,u}, \\
x_t &= x_{t-\Delta t} + \kappa_x \int_{t-\Delta t}^{t} (\bar{x} - \mu_u) du + \sigma_x \int_{t-\Delta t}^{t} dB_{x,u}.
\end{aligned}$$

Note that an Ito integral is a martingale and, hence, its conditional mean is zero. By taking the conditional expectations $\mathbb{E}_{t-\Delta t}[\cdot]$ on both sides of the equations, we simply obtain $\mathbb{E}_{t-\Delta t}[S_t] = \eta + \Psi S_{t-\Delta t}$, where

$$\begin{aligned}
\eta &= \begin{bmatrix}
-\frac{\kappa_\lambda \bar{\xi}}{\kappa_\lambda - \kappa_\xi} \left(e^{-\kappa_\xi \Delta t} - e^{-\kappa_\lambda \Delta t}\right) + \bar{\xi}\left(1 - e^{-\kappa_\lambda \Delta t}\right) \\
\bar{\xi}\left(1 - e^{-\kappa_\xi \Delta t}\right) \\
\bar{\mu}\left(1 - e^{-\kappa_\mu \Delta t}\right) \\
\bar{x}\left(1 - e^{-\kappa_x \Delta t}\right)
\end{bmatrix}, \\
\Psi &= \begin{bmatrix}
e^{-\kappa_\lambda \Delta t} & \frac{\kappa_\lambda}{\kappa_\lambda - \kappa_\xi}\left(e^{-\kappa_\xi \Delta t} - e^{-\kappa_\lambda \Delta t}\right) & 0 & 0 \\
0 & e^{-\kappa_\xi \Delta t} & 0 & 0 \\
0 & 0 & e^{-\kappa_\mu \Delta t} & 0 \\
0 & 0 & 0 & e^{-\kappa_x \Delta t}
\end{bmatrix}.
\end{aligned}$$

This relation allows us to express S_t as in equation (13):

$$S_t = \mathbb{E}_{t-\Delta t}[S_t] + \epsilon_t, \quad \text{where } \mathbb{E}_{t-\Delta t}[\epsilon_t] = 0 \text{ and } \mathrm{Var}_{t-\Delta t}[\epsilon_t] = \Omega_{t-\Delta t},$$

where the 4×4 covariance matrix $\Omega_{t-\Delta t}$ is given by

$$\Omega_{t-\Delta t} = \begin{bmatrix} \Omega_{\lambda\lambda,t-\Delta t} & \Omega_{\lambda\xi,t-\Delta t} & 0 & 0 \\ \Omega_{\lambda\xi,t-\Delta t} & \Omega_{\xi\xi,t-\Delta t} & 0 & 0 \\ 0 & 0 & \Omega_{\mu\mu,t-\Delta t} & 0 \\ 0 & 0 & 0 & \Omega_{xx,t-\Delta t} \end{bmatrix}.$$

Clearly, ϵ_t is non-normal. However, in order to use a conventional filtering approach, we approximate it by a mean-zero normal random variable with the same covariance matrix $\Omega_{t-\Delta t}$.[1] We find each element of $\Omega_{t-\Delta t}$ by considering the marginal and joint dynamics of λ_t, ξ_t, μ, and x_t:

$$\begin{aligned}
\Omega_{\lambda\lambda,t-\Delta t} &= \frac{\kappa_\lambda^2\sigma_\xi^2\xi_{t-\Delta t}}{(\kappa_\lambda-\kappa_\xi)^2\kappa_\xi}\left(e^{-\kappa_\xi\Delta t}-e^{-2\kappa_\xi\Delta t}\right)+\frac{\kappa_\lambda^2\bar{\xi}\sigma_\xi^2}{2(\kappa_\lambda-\kappa_\xi)^2\kappa_\xi}\left(1-e^{-\kappa_\xi\Delta t}\right)^2 \\
&\quad-\frac{2\kappa_\lambda\sigma_\xi^2(\xi_{t-\Delta t}-\bar{\xi})}{(\kappa_\lambda-\kappa_\xi)^2}\left(e^{-\kappa_\xi\Delta t}-e^{-(\kappa_\lambda+\kappa_\xi)\Delta t}\right)-\frac{2\kappa_\lambda^2\sigma_\xi^2\bar{\xi}}{(\kappa_\lambda-\kappa_\xi)^2(\kappa_\xi+\kappa_\lambda)}\left(1-e^{-(\kappa_\lambda+\kappa_\xi)\Delta t}\right) \\
&\quad+\frac{\kappa_\lambda^2\sigma_\xi^2(\xi_{t-\Delta t}-\bar{\xi})}{(\kappa_\lambda-\kappa_\xi)^2(2\kappa_\lambda-\kappa_\xi)}\left(e^{-\kappa_\xi\Delta t}-e^{-2\kappa_\lambda\Delta t}\right)+\frac{\kappa_\lambda\sigma_\xi^2\bar{\xi}}{2(\kappa_\lambda-\kappa_\xi)^2}\left(1-e^{-2\kappa_\lambda\Delta t}\right) \\
&\quad+\frac{(\lambda_{t-\Delta t}-\bar{\xi})\sigma_\lambda^2}{\kappa_\lambda}\left(e^{-\kappa_\lambda\Delta t}-e^{-2\kappa_\lambda\Delta t}\right)+\frac{\kappa_\lambda(\xi_{t-\Delta t}-\bar{\xi})\sigma_\lambda^2}{(\kappa_\lambda-\kappa_\xi)(2\kappa_\lambda-\kappa_\xi)}\left(e^{-\kappa_\xi\Delta t}-e^{-2\kappa_\lambda\Delta t}\right) \\
&\quad-\frac{(\xi_{t-\Delta t}-\bar{\xi})\sigma_\lambda^2}{\kappa_\lambda-\kappa_\xi}\left(e^{-\kappa_\lambda\Delta t}-e^{-2\kappa_\lambda\Delta t}\right)+\frac{\bar{\xi}\sigma_\lambda^2}{2\kappa_\lambda}\left(1-e^{-2\kappa_\lambda\Delta t}\right), \\
\Omega_{\xi\xi,t-\Delta t} &= \frac{\sigma_\xi^2\xi_{t-\Delta t}}{\kappa_\xi}\left(e^{-\kappa_\xi\Delta t}-e^{-2\kappa_\xi\Delta t}\right)+\frac{\sigma_\xi^2\bar{\xi}}{2\kappa_\xi}\left(1-e^{-\kappa_\xi\Delta t}\right)^2, \\
\Omega_{\lambda\xi,t-\Delta t} &= \frac{\kappa_\lambda}{\kappa_\lambda-\kappa_\xi}\Omega_{\xi\xi,t-\Delta t} \\
&\quad-\frac{\sigma_\xi^2\left(\xi_{t-\Delta t}-\bar{\xi}\right)}{\kappa_\lambda-\kappa_\xi}\left(e^{-\kappa_\xi\Delta t}-e^{-(\kappa_\lambda+\kappa_\xi)\Delta t}\right)-\frac{\kappa_\lambda\sigma_\xi^2\bar{\xi}}{(\kappa_\lambda-\kappa_\xi)(\kappa_\lambda+\kappa_\xi)}\left(1-e^{-(\kappa_\xi+\kappa_\lambda)\Delta t}\right), \\
\Omega_{\mu\mu,t-\Delta t} &= \frac{\sigma_\mu^2}{2\kappa_\mu}\left(1-e^{-2\kappa_\mu\Delta t}\right), \\
\Omega_{xx,t-\Delta t} &= \frac{\sigma_x^2}{2\kappa_x}\left(1-e^{-2\kappa_x\Delta t}\right).
\end{aligned}$$

Since our measurement equation is not linear in the state variables, we adopt the unscented

[1] As discussed in Section 3.2, it is well known that the effect of this approximation is minimal.

Kalman filter. The predicted state vector and its variance at time $t - \Delta t$ (i.e., $\hat{S}_{t|t-\Delta t}$ and $P_{t|t-\Delta t}$) are given as follows:

$$\begin{aligned} \hat{S}_{t|t-\Delta t} &= \eta + \Psi \hat{S}_{t-\Delta t}, \\ P_{t|t-\Delta t} &= \Psi P_{t-\Delta t} \Psi' + \Omega_{t-\Delta t}. \end{aligned}$$

We define sigma points that help capture the mean and variance of the latent state variables. Specifically, we select the following set of $2L + 1$ sigma points ($\mathcal{S}$) and weights (W^m for the mean and W^c for the covariance of the observations evaluated at the sigma points):

$$\begin{aligned} \mathcal{S}_0 &= \hat{S}_{t|t-\Delta t}, \\ \mathcal{S}_i &= \hat{S}_{t|t-\Delta t} + \left(\sqrt{(L+\chi)P_{t|t-\Delta t}}\right)_i, \quad i = 1, \cdots, L, \\ \mathcal{S}_i &= \hat{S}_{t|t-\Delta t} - \left(\sqrt{(L+\chi)P_{t|t-\Delta t}}\right)_{i-L}, \quad i = L+1, \cdots, 2L, \end{aligned}$$

and

$$\begin{aligned} W_0^m &= \frac{\chi}{L+\chi}, \\ W_0^c &= \frac{\chi}{L+\chi} + (1 - \alpha^2 + \beta), \\ W_i^m = W_i^c &= \frac{1}{2(L+\chi)}, \quad i = 1, \cdots, 2L, \end{aligned}$$

where L is the number of the latent variables, $\chi = \alpha^2(L + \kappa) - L$ is a scaling parameter, and $\left(\sqrt{(L+\chi)P_{t|t-\Delta t}}\right)_i$ is the i-th column of the matrix square root. In this paper, we use $\alpha = 0.01$, $\beta = 2$, and $\kappa = 0$.

The mean and covariance of the predicted vector $\hat{Y}_t$ are computed using a weighted mean

and covariance of the sigma points:

$$\begin{aligned}
\hat{Y}_{t|t-\Delta t} &= \sum_{i=0}^{2L} W_i^m h(\mathcal{S}_i), \\
P^y_{t|t-\Delta t} &= \sum_{i=0}^{2L} W_i^c \left(h(\mathcal{S}_i) - \hat{Y}_{t|t-\Delta t}\right)\left(h(\mathcal{S}_i) - \hat{Y}_{t|t-\Delta t}\right)' + Q.
\end{aligned}$$

Then, we obtain the filtered state vector at time t (i.e., $\hat{S}_t$) as follows:

$$\begin{aligned}
\hat{S}_t &= \hat{S}_{t|t-\Delta t} + K_t \hat{e}_t, \\
P_t &= P_{t|t-\Delta t} - K_t P^y_{t|t-\Delta t} K_t',
\end{aligned}$$

where

$$\begin{aligned}
K_t &= \sum_{i=0}^{2L} W_i^c \left(\mathcal{S}_i - \hat{S}_{t|t-\Delta t}\right)\left(h(\mathcal{S}_i) - \hat{Y}_{t|t-\Delta t}\right)' \left(P^y_{t|t-\Delta t}\right)^{-1}, \\
\hat{e}_t &= Y_t - \hat{Y}_{t|t-\Delta t}.
\end{aligned}$$

For the initial month, the values of $\hat{S}_{t-\Delta t}$ and $P_{t-\Delta t}$ are set to be the unconditional mean and variance of S_t. The Kalman filter recursion also enables us to calculate the likelihood of observing Y_t conditional on $Y_{t-\Delta t}$:

$$\log \mathcal{L}_t = -\frac{l}{2}\log(2\pi) - \frac{1}{2}\log|P^y_{t|t-\Delta t}| - \frac{1}{2}\hat{e}_t' \left(P^y_{t|t-\Delta t}\right)^{-1} \hat{e}_t,$$

where l is the size of the vector Y_t.

C Estimation of nested models

The key feature of our model is disaster risk, which consists of time-varying short-run and long-run components. To demonstrate the importance of disaster risk, we examine two nested cases: (i) constant long-run mean of disaster risk (i.e., no variation in ξ_t) where $\kappa_\xi = \sigma_\xi = \delta_\xi = \theta_\xi = 0$; (ii) constant disaster risk (i.e., no variation in λ_t) where $\kappa_\xi = \kappa_\lambda = \sigma_\xi = \sigma_\lambda = \delta_\xi = \delta_\lambda = \theta_\xi = \theta_\lambda = 0$. It is important to note that we do not consider a specification without disaster risk (no jump component at all) because, in the absence of disaster risk, the interbank rate would collapse to the OIS rate under our model setup. Parameter estimates for both alternative models are presented in the tables below:

Nested case (i): Constant long-run mean of disaster risk

		κ_μ	σ_μ	σ_C	$\bar{\mu}$
Consumption growth	Est.	0.0687	0.0035	0.0078	0.0105
	(SE)	(0.0003)	(0.0000)	(0.0001)	
		κ_q	σ_q	$\bar{q}$	
Expected inflation	Est.	0.5239	0.0065	0.0212	
	(SE)	(0.3153)	(0.0011)	(0.0028)	
		κ_λ	σ_λ	$\bar{p}$	$\bar{\xi}$
Disaster risk	Est.	0.4252	0.1385	0.9214	0.0286
	(SE)	(0.0030)	(0.0003)	(0.0076)	
		κ_x	σ_x	$\bar{x}$	
Convenience yield	Est.	0.8162	0.0017	0.0021	
	(SE)	(0.1915)	(0.0003)	(0.0004)	
		δ_λ	δ_q	δ_μ	δ_0
Short rate	Est.	-0.1004	0.4253	2.4470	-0.0174
	(SE)	(0.0005)	(0.0024)	(0.0224)	
		θ_λ	θ_q	θ_μ	θ_N
Market price of risk	Est.	-0.1381	-4.2443	0.1968	-0.1699
	(SE)	(0.0005)	(0.0288)	(0.0008)	(0.0009)
		σ_{SP}	σ_{ITR}	σ_{OPT}	
Measurement errors	Est.	0.0016	0.0033	0.0745	
	(SE)	(0.0000)	(0.0000)	(0.0007)	

One notable observation from the estimation of these two nested models is that the parameter estimates of κ_μ are much smaller than that in our main specification in Table 2. These estimates are around 0.05, which is similar to the estimate of κ_ξ in Table 2. This finding suggests that a very highly persistent state variable is required to capture the time

Nested case (ii): Constant disaster risk

		κ_μ	σ_μ	σ_C	$\bar{\mu}$
Consumption growth	Est.	0.0435	0.0042	0.0077	0.0105
	(SE)	(0.0007)	(0.0001)	(0.0001)	
		κ_q	σ_q	$\bar{q}$	
Expected inflation	Est.	0.5239	0.0065	0.0212	
	(SE)	(0.3153)	(0.0011)	(0.0028)	
		$\bar{p}$	$\bar{\xi}$		
Disaster risk	Est.	0.8496	0.0286		
	(SE)	(0.0063)			
		κ_x	σ_x	$\bar{x}$	
Convenience yield	Est.	0.8162	0.0017	0.0021	
	(SE)	(0.1915)	(0.0003)	(0.0004)	
		δ_q	δ_μ	δ_0	
Short rate	Est.	0.5744	2.1526	-0.0203	
	(SE)	(0.0077)	(0.0461)		
		θ_q	θ_μ	θ_N	
Market price of risk	Est.	-2.8155	0.1174	-0.0880	
	(SE)	(0.0415)	(0.0011)	(0.0005)	
		σ_{SP}	σ_{ITR}	σ_{OPT}	
Measurement errors	Est.	0.0038	0.0039	0.0736	
	(SE)	(0.0000)	(0.0003)	(0.0010)	

series of interest rates and option-implied volatilities. Since ξ_t is no longer time-varying in the nested models, the persistence of μ_t is artificially forced to be very high. The omission of time-varying ξ_t increases the measurement error in interest rates by 13 to 19 basis points. When λ_t is held constant, the measurement error in interest rate spreads more than doubles.

In addition to the two cases related to disaster risk, we consider a third nested model: (iii) absence of expected inflation, where we set $\kappa_q = \sigma_q = \bar{q} = \delta_q = \theta_q = 0$. While expected inflation plays a crucial role in capturing the level of interest rates in the full model, its omission is not impossible given the reduced-form nature of our framework. The corresponding parameter estimates are reported in the table below.

Given that these alternative models are nested within our main model specification, we conduct a likelihood ratio test to compare their performance. The table below reports the log-likelihood for the full model alongside those for the three nested models. Under the null of no difference between the main model and each nested model, the likelihood ratio test statistic $2 \times (\log \mathcal{L} - \log \mathcal{L}_{\text{nested}})$ should follow a chi-square distribution with degrees of freedom equal

Nested case (iii): Absence of expected inflation

		κ_μ	σ_μ	σ_C	$\bar{\mu}$
Consumption growth	Est.	0.5799	0.0056	0.0086	0.0105
	(SE)	(0.0098)	(0.0002)	(0.0001)	
		κ_ξ	σ_ξ	$\bar{\xi}$	
	Est.	0.0442	0.0215	0.0286	
Disaster risk	(SE)	(0.0009)	(0.0001)		
		κ_λ	σ_λ	$\bar{p}$	
	Est.	0.4472	0.1749	0.8824	
	(SE)	(0.0067)	(0.0006)	(0.0220)	
		κ_x	σ_x	$\bar{x}$	
Convenience yield	Est.	0.8162	0.0017	0.0021	
	(SE)	(0.1915)	(0.0003)	(0.0004)	
		δ_λ	δ_ξ	δ_μ	δ_0
Short rate	Est.	-0.1294	-2.1165	1.9295	0.0581
	(SE)	(0.0020)	(0.0119)	(0.0087)	
		θ_λ	θ_ξ	θ_μ	θ_N
Market price of risk	Est.	-0.1190	-0.2655	0.1015	-0.1386
	(SE)	(0.0008)	(0.0008)	(0.0027)	(0.0035)
		σ_{SP}	σ_{ITR}	σ_{OPT}	
Measurement errors	Est.	0.0014	0.0022	0.0776	
	(SE)	(0.0000)	(0.0000)	(0.0007)	

to the number of restrictions. The table shows that the resulting p-values are virtually zero, rejecting the nested models and thereby supporting our original specification.

	Main	(i) Constant ξ	(ii) Constant λ	(iii) Without q
$\log \mathcal{L}$	26,741.17	25,160.56	23,897.70	26,386.13
p-value		0.00	0.00	0.00

D Equivalent bond price volatility

In Figure 3, the Black-implied volatilities for the 2-year cap are generally much higher than those for the 5-year cap. Furthermore, in all of the panels in Figure 3, the Black-implied volatilities between 2010 and 2016 are exceptionally high even compared to the Great Recession period between 2007 and 2009.

Why do the time series and cross sectional patterns of Black-implied volatilities seem odd? The reason is that Black-implied volatilities for caps and swaptions, converted from their market prices through the Black formulas, represent yield volatilities, not bond price volatilities. Hence, the level of Black-implied volatilities simply tends to be higher when the level of interest rates is lower. This explains why Black-implied volatilities in the data turn out to be so high in the post Great Recession period despite relatively lower uncertainty in the market: a 1% expected movement in a yield corresponds to 20% yield volatility if the yield is currently at 5%, whereas it corresponds to 100% if the yield is at 1%.

To facilitate interpretation, it is possible to convert each Black-implied volatility into its equivalent price volatility. Under the Black model, forward yield volatility σ_{yield} shares the following relation with forward-starting bond price volatility σ_{price}:

$$\sigma_{\text{price}} = \tau \times y \times \sigma_{\text{yield}},$$

where, with a slight abuse of notation, τ is the maturity of the bond and y is the given (forward) yield. Using this simple relation, we can covert the Black-implied volatilities in the data and in the model into their equivalent forward-starting bond price volatilities.

The figure below plots the time series of the equivalent bond price volatilities for the 2-, 3-, and 5-year caps (Panels A, B, and C) and those for the 1-into-4, 2-into-3, and 4-into-1 swaptions (Panels D, E, and F) in the data (solid blue lines) and in the model (dashed red lines). The Black-implied volatility for the T-maturity cap is converted into the price volatility of a bond that corresponds to its last caplet: a 6-month zero-coupon bond starting after $(T - 0.5)$ years and maturing after T years from today. The Black-implied volatility for

the T-into-$\bar{T}$ swaption is converted to the price volatility of a $\bar{T}$-maturity zero-coupon bond starting T years from today. The sample period is from February 2002 to December 2019.

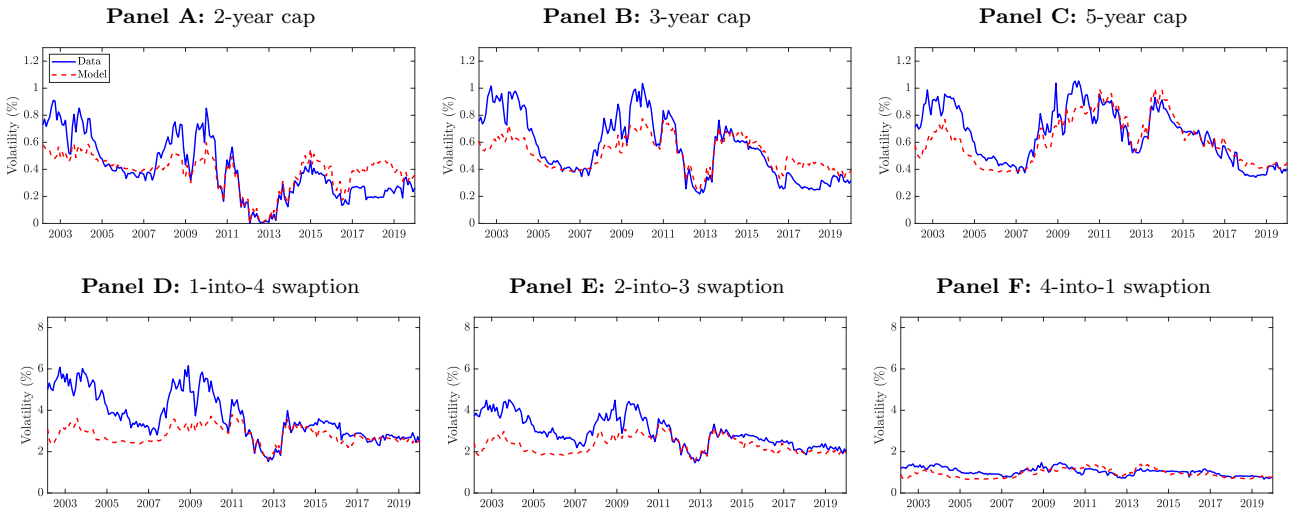

E Filtered time series of x_t and μ_t

The figure below presents the filtered time series of the instantaneous convenience rate x_t (Panel A) and mean consumption growth per month $\mu_t/12$ (Panel B) from February 2002 to December 2019. In Panel B, we overlay the time series of monthly mean consumption growth (solid blue line) with that of monthly realized consumption growth (dashed red line). Summary statistics for each time series are also reported.

Panel A: Convenience rate

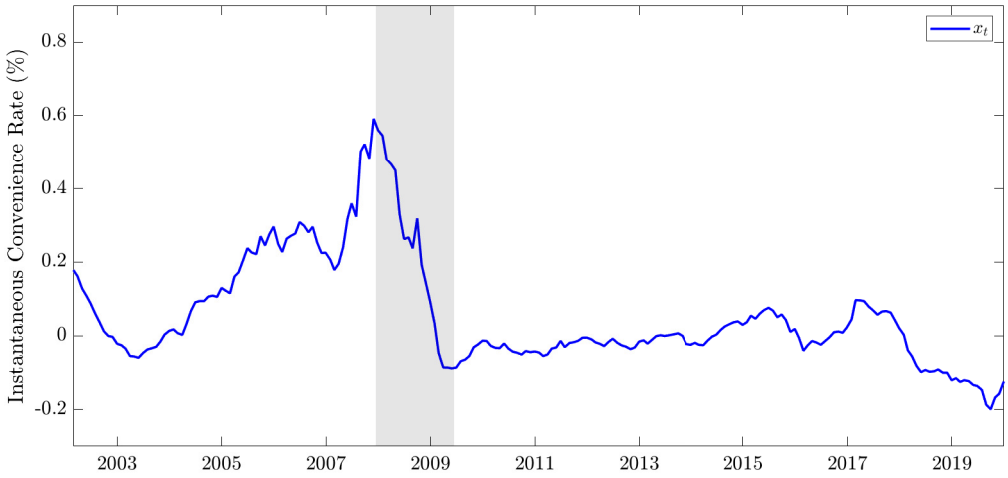

Panel B: Consumption growth

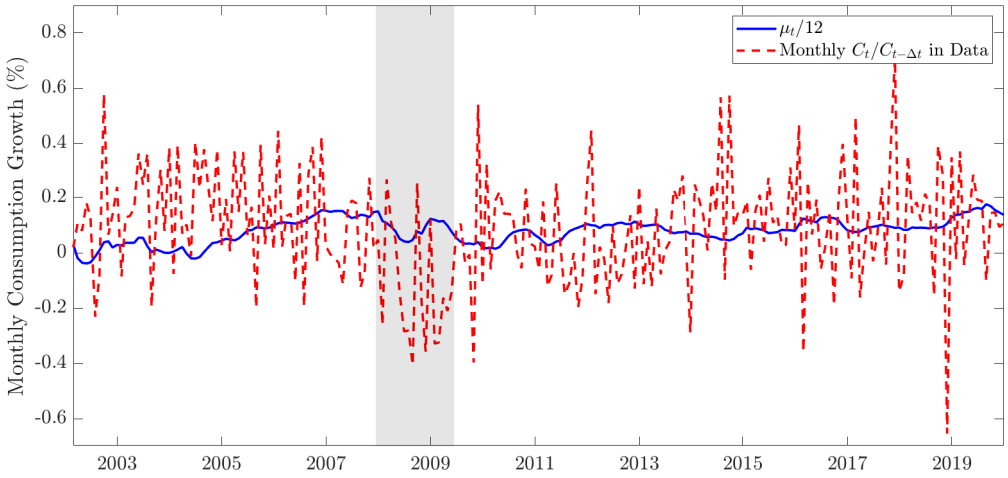

	Mean	SD	Min	5th	50th	95th	Max
x	0.06	0.15	-0.20	-0.12	0.00	0.33	0.59
μ	0.94	0.53	-0.46	0.01	1.00	1.81	2.11

F COVID-19 pandemic crisis

In 2020, the global economy and financial markets were severely impacted by the COVID-19 pandemic crisis. What do interbank rates and their options imply about this crisis through our model framework?

We extend our data sample and examine how the implied short-run and long-run components of disaster risk progressed over the pandemic period. Based on the estimated parameters in Table 2, we apply the unscented Kalman filter from Section 3.2 to the additional data from January 2020 to December 2020. The figure below plots the resulting time series of filtered λ_t (solid blue line) and ξ_t (dashed red line).

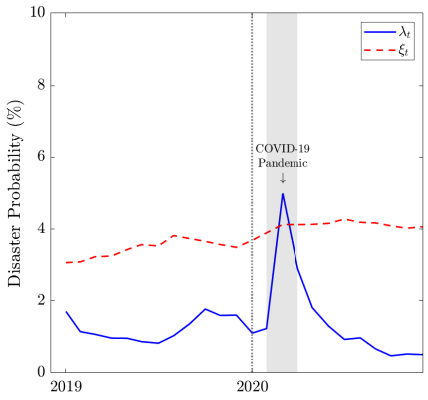

The figure reveals that the long-run component ξ_t slightly increased at the onset of the crisis and remained elevated throughout 2020 (4.1% in December). In contrast, the short-run component λ_t exhibited drastic changes over the period. Until February, λ_t stayed at a low level of around 1%, but it jumped up to 5.0% in March. This was followed by an abrupt decline in April and May, pushing λ_t quickly back to its pre-pandemic level. Overall, the figure suggests that, at least through our model framework, the COVID-19 pandemic resulted in a very short-lived economic/financial crisis, despite its long-lasting impacts. This interpretation is in line with the view of the Business Cycle Dating Committee of the NBER; the committee determined that the pandemic-originated recession only lasted for two months (March and April), making it the shortest U.S. recession ever documented.

G Structure of bond price volatility

In our model, the bond volatility is a function of the two disaster state variables λ_t and ξ_t. More formally, let $P_i(t, t+\tau)$ denote the price of a zero-coupon interbank lending where τ is the bond maturity. By Ito's lemma, the price dynamics under the physical measure can be expressed as follows:

$$\frac{dP_{i,t}}{P_{i,t^-}} = \mu_{P_i,t}dt + b_{i,\lambda}(\tau)\sigma_\lambda\sqrt{\lambda_t}dB_{\lambda,t} + b_{i,\xi}(\tau)\sigma_\xi\sqrt{\xi_t}dB_{\xi,t} + b_{i,\mu}(\tau)\sigma_\mu dB_{\mu,t} + b_{i,q}(\tau)\sigma_q dB_{q,t} + \left(e^{b_{i,q}(\tau)Z_{q,t}} - 1\right)dN_t.$$

This implies that the instantaneous bond volatility is calculated by

$$\frac{d\text{Var}_t(\log P_{it})}{dt} = \underbrace{\left(b_{i,q}^2(\tau)\sigma_q^2 + b_{i,\mu}^2(\tau)\sigma_\mu^2\right)}_{\varphi_0(\tau)} + \underbrace{\left(b_\lambda^2(\tau)\sigma_\lambda^2 + b_{i,q}^2(\tau)E_t\left[Z_{q,t}^2\right]\right)}_{\varphi_\lambda(\tau)}\lambda_t + \underbrace{b_\xi^2(\tau)\sigma_\xi^2}_{\varphi_\xi(\tau)}\xi_t.$$

The figure below plots the two factor loadings $\varphi_\lambda(\tau)$ and $\varphi_\xi(\tau)$, as well as the intercept term $\varphi_0(\tau)$, as functions of τ. While we can see that the intercept term is very small and does not vary much with maturity (Panel A), the two factor loadings increase monotonically (Panels B and C). Comparing the two, the factor loading for ξ_t rises much faster with a steeper slope than that for λ_t. The rate of increase is also larger; $\varphi_\xi(\tau)$ is convex in τ, whereas $\varphi_\lambda(\tau)$ is concave. This is intuitive since the long-run component of disaster risk has a greater effect on long-term rates, which leads to a larger impact on the variance of long-term bonds.

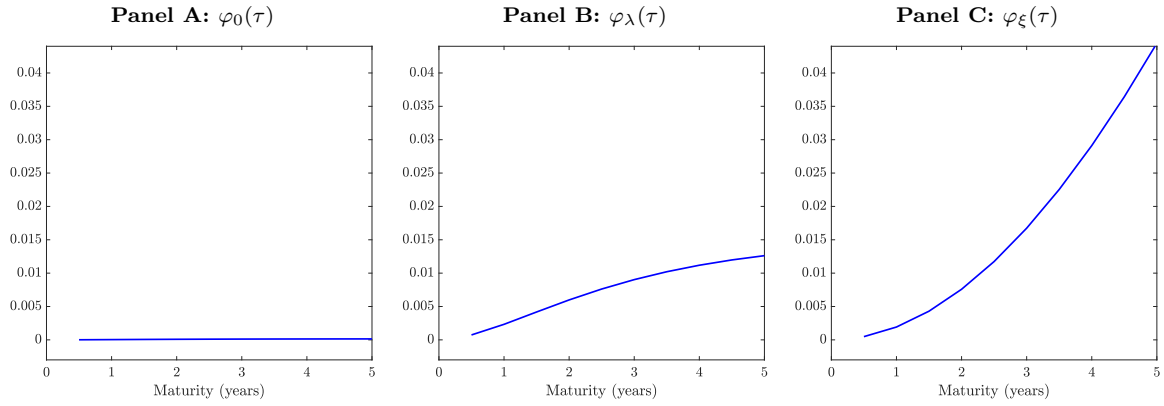

References for the Internet Appendix

Bakshi, Gurdip, John Crosby, Xiaohui Gao, and Jorge W. Hansen, 2023, Treasury option returns and models with unspanned risks, *Journal of Financial Economics* 150, 103736.

Bakshi, Gurdip, Xiaohui Gao, and Jinming Xue, 2023, Recovery with applications to forecasting equity disaster probability and testing the spanning hypothesis in the treasury market, *Journal of Financial and Quantitative Analysis* pp. 1–35.

Berkman, Henk, Ben Jacobsen, and John B. Lee, 2011, Time-varying rare disaster risk and stock returns, *Journal of Financial Economics* 101, 313–332.

Gabaix, Xavier, 2012, An exactly solved framework for ten puzzles in macro-finance, *Quarterly Journal of Economics* 127, 645–700.

Han, Bing, 2007, Stochastic volatilities and correlations of bond yields, *Journal of Finance* 62, 1491–1524.

Longstaff, Francis A., Pedro Santa-Clara, and Eduardo S. Schwartz, 2001, The relative valuation of caps and swaptions: Theory and empirical evidence, *Journal of Finance* 56, 2067–2109.

Manela, Asaf, and Alan Moreira, 2017, News implied volatility and disaster concerns, *Journal of Financial Economics* 123, 137–162.

Seo, Sang Byung, and Jessica A. Wachter, 2018, Do rare events explain CDX tranche spreads?, *Journal of Finance* 73, 2343–2383.

Trolle, Anders B., and Eduardo S. Schwartz, 2009, Unspanned stochastic volatility and the pricing of commodity derivatives, *Review of Financial Studies* 22, 4423–4461.

Tsai, Jerry, 2015, Rare disasters and the term structure of interest rates, Working paper.

Wachter, Jessica A., 2013, Can time-varying risk of rare disasters explain aggregate stock market volatility?, *Journal of Finance* 68, 987–1035.